Dynamics of dense electronegative low density lipoproteins and their preferential association with lipoprotein phospholipase A_2

John W. Gaubatz, Baiba K. Gillard, John B. Massey, Ron C. Hoogeveen, Max Huang, Eric E. Lloyd, Joe L. Raya, Chao-yuh Yang, and Henry J. Pownall[1]

Section of Atherosclerosis and Lipoprotein Research, Department of Medicine, Baylor College of Medicine, Houston, TX 77030

Abstract **Small, dense, electronegative low density lipoprotein [LDL(−)] is increased in patients with familial hypercholesterolemia and diabetes, populations at increased risk for coronary artery disease. It is present to a lesser extent in normolipidemic subjects. The mechanistic link between small, dense LDL(−) and atherogenesis is not known. To begin to address this, we studied the composition and dynamics of small, dense LDL(−) from normolipidemic subjects. NEFA levels, which correlate with triglyceride content, are quantitatively linked to LDL electronegativity. Oxidized LDL is not specific to small, dense LDL(−) or lipoprotein [a] (i.e., abnormal lipoprotein). Apolipoprotein C-III is excluded from the most abundant LDL (i.e., that of intermediate density: 1.034 < d < 1.050 g/ml) but associated with both small and large LDL(−). In contrast, lipoprotein-associated phospholipase A_2 ($LpPLA_2$) is highly enriched only in small, dense LDL(−).** **The association of $LpPLA_2$ with LDL may occur through amphipathic helical domains that are displaced from the LDL surface by contraction of the neutral lipid core.—**Gaubatz, J. W., B. K. Gillard, J. B. Massey, R. C. Hoogeveen, M. Huang, E. E. Lloyd, J. L. Raya, C-y. Yang, and H. J. Pownall. **Dynamics of dense electronegative low density lipoproteins and their preferential association with lipoprotein phospholipase A_2.** ***J. Lipid Res.*** **2007.** 48: **348–357.**

Supplementary key words atherogenesis • fatty acid • apo B-100

Although low density lipoprotein-cholesterol is a risk factor for cardiovascular disease, an expanding body of evidence suggests that one or more minor LDL subfractions serve as the atherogenic agent. One hypothesis is that LDL enters the arterial wall, where its lipids are oxidatively modified, thereby initiating a series of biochemical processes that culminate in lesion formation (1). Nonetheless, modified LDL present in the circulation also has atherogenic properties (2), as indicated by the correlation of atherosclerosis with levels of oxidized plasma LDL (3–5). Plasma contains several forms of modified LDL, including heterogeneously oxidized LDL (6), glycated LDL from diabetic subjects (7), and desialylated LDL (8). Importantly, plasma from both normal and dyslipidemic patients contains electronegative low density lipoprotein [LDL(−)] (9); however, there have been few comprehensive studies of LDL(−) in normolipidemic subjects.

Plasma LDL(−) is increased in subjects at high risk for cardiovascular disease as a result of hypercholesterolemia (10–12), hypertriglyceridemia (11, 13), diabetes (14–17), or coronary artery disease (18). Simvastatin therapy reduces the proportion of LDL(−) without modifying its oxidizability (12). Relative to normal LDL, LDL(−) has *1*) lower vitamin E content; *2*) increased lipid peroxidation, as assessed by thiobarbituric acid-reactive substances and conjugated dienes; *3*) more highly aggregated apolipoprotein B (apoB); *4*) reduced affinity for the LDL receptor; *5*) greater density and is more readily oxidized; and *6*) higher lipoperoxide content (9, 19–22). Other studies have shown that the cytotoxicity of LDL(−) to endothelial cells is independent of its oxidation and peroxidation (23–28). Thus, questions remain regarding the composition and properties of LDL(−) and their relationship to pathogenicity. Although there have been a few studies of LDL(−) in normolipidemic subjects, none has elucidated LDL structure in situations of minimal lipoprotein modification, a condition potentially preceding the formation of more severely modified, and patently atherogenic, particles. Given the association of LDL(−) with several pathological states, it is important to fully characterize the properties of LDL(−). Here, we provide a detailed physical and chemical analysis of LDL(−) derived from normolipidemic subjects.

Manuscript received 7 June 2006 and in revised form 27 October 2006.

Published, JLR Papers in Press, November 13, 2006.
DOI 10.1194/jlr.M600249-JLR200

[1] To whom correspondence should be addressed.
e-mail: hpownall@bcm.tmc.edu

METHODS

LDL subfractionation by density

Plasma was isolated from blood obtained through the Methodist Hospital Blood Donor Center, where each participant provided informed consent. All patient protocols were approved by the institutional review board. The Lipid Laboratory of Baylor College of Medicine used accepted methodologies to analyze plasma triglyceride and cholesterol. None of the volunteers was overtly dyslipidemic. The respective means and (SEM) for total cholesterol and triglyceride were 138 (5) and 118 (12) mg/dl; ranges were 112–193 and 44–255 mg/dl.

LDL was isolated from donor plasma via sequential flotation in solutions adjusted to the respective densities of 1.006, 1.019, and 1.063 g/ml by the addition of KBr (29). LDL (4 ml) from the flotation at d = 1.063 g/ml was transferred to the bottom of 14 × 95 mm SW40 centrifuge tubes (Beckman Coulter, Fullerton CA). LDL was sequentially overlaid with 2 ml each of saline adjusted with KBr to densities of 1.055, 1.050, 1.040, and 1.030. LDL was ultracentrifuged in a Beckman SW40 Ti swinging-bucket rotor at 35,000 rpm for 48 h at 4°C, after which each tube was marked along its length using a template to guide fractionation. Guided by the marks, fractions were collected by aspiration with a Pasteur pipette. The top 0.5 ml was discarded, and seven fractions (1.4 ml) increasing in density from D1 to D7 were collected. The bottom 1.0 ml (i.e., infranatant) was collected but not included in the LDL fractions. The densities of each fraction were determined by pycnometry of similarly treated tube contents (n = 3), which reflected the same gradient of KBr without LDL.

Agarose gel electrophoresis

The LDL density subfractions were analyzed by electrophoresis in 0.7% agarose (90 mM Tris, 80 mM borate, pH 8.2). LDL samples (2–10 μg of protein in <20 μl) were loaded onto the gels, and electrophoresis was performed at 4°C at 90 V for 90 min.

Anion-exchange analysis of LDL

Using an Amersham/Pharmacia ÄKTA Chromatography System and a Mono Q 5/50 GL column (Amersham/Pharmacia), LDL subfractions were isolated according to density and separated on the basis of particle charge (13, 30). Fractionation was achieved using a flow rate of 1 ml/min and a linear gradient of 0–0.1 M NaCl (10 min) followed by 0.2, 0.3, and 1 M, then re-equilibrated to 0 M NaCl in 10 mM Tris, 0.5 mM EDTA (pH 7.4) for 8, 6, 5, and 6 min, respectively. Taking absorbance values at 280 nm, this program yielded electropositive and electronegative fractions [LDL(+) and LDL(−)] at 0.2 and 0.3 M NaCl, respectively; their relative abundance was determined via peak integration software supplied with the system. In some experiments, LDL(+) and LDL(−) were collected in 1 ml fractions and concentrated with Centriprep filters (YM-100; Millipore). Isolated fractions were stored at 4°C until needed for further analysis.

SDS-PAGE

LDL subfractions were delipidated with ethyl acetate-ethanol (1:1), solubilized with 10% SDS, and separated on 4–15% SDS gels (Bio-Rad Laboratories) at 4°C at 100 V for 2 h.

Lipid-free human serum albumin

Scavenging of monoacyl lipids required punctiliously NEFA-free human serum albumin (HSA). Nominally NEFA-free HSA (Sigma-Aldrich, St. Louis, MO) was additionally extracted with Folch reagent (31) to remove adventitious lipid.

Immunoanalysis of lipoprotein-associated phospholipase A_2 and apoC-III

After electrophoresis of LDL subfractions on agarose or SDS-polyacrylamide gels and electrotransfer onto polyvinylidene difluoride membranes (Bio-Rad), blots were blocked with Tris-buffered saline containing 0.05% (v/v) Tween-20 and 3% (w/v) nonfat dry milk. Probing was performed overnight at 4°C with polyclonal goat antibody to apoC-III (1:1,000 dilution; Academy Biomedical Co., Houston, TX) or for 1 h at room temperature with polyclonal rabbit anti-human lipoprotein-associated phospholipase A_2 ($LpPLA_2$) (1:2,500 dilution; Cayman Chemical, Ann Arbor, MI). After washing the membranes four times in 10 mmol/l Tris-HCl, 150 mM NaCl, and 0.05% Tween-20 (pH 7.5), a secondary HRP-conjugated donkey anti-goat antibody (Jackson ImmunoResearch Laboratories; apoC-III) or HRP-conjugated goat anti-rabbit antibody (Bio-Rad; $LpPLA_2$) was incubated at 1:1,000 at room temperature for 1 h. The membrane was washed and immunoreactive bands were detected via chemiluminescence using the ECL Plus Western blotting detection system (GE Healthcare). The blots were exposed to CL-X film (Pierce) for 1–10 min. $LpPLA_2$ mass was also quantified using a commercial PLAC™ kit (diaDexus, San Francisco, CA) that is based on a sandwich ELISA using two monoclonal antibodies (32).

Lipid analysis

Lipids were extracted from LDL in accordance with Folch, Lees, and Sloane Stanley (31). The free cholesterol (FC), phospholipid, NEFA, and triglyceride were determined using enzyme-based kits (Wako Chemicals USA, Richmond, VA). Total cholesterol was determined after treating samples with a cholesteryl esterase. Cholesteryl ester (CE) was measured by calculating the difference between total cholesterol and FC multiplied by 1.68. Protein was determined as described by Lowry et al. (33). Oxidized LDL levels (n = 4) were measured via direct sandwich ELISA (Mercodia, Winston-Salem, NC) based on the capture of monoclonal antibody 4E6, which detects oxidatively modified apoB. The values were normalized to protein concentrations of 1 mg/ml (34). LDL size was calculated in accordance with Sherman et al. (35) using the partial specific volumes of each of the components, as reported by Tardieu et al. (36), and their respective molar ratios relative to apoB-100, which is assumed to have a partial specific volume of 0.73 ml/g and to occur in LDL at only one copy per particle.

NEFA acyl chain compositions were determined by mass spectrometry of their fatty acid methyl esters, after separation by gas chromatography (37). As an internal standard, heptadecanoic acid (1 μg) was dissolved in 5 ml of methylating reagent (2% acetyl chloride in methanol), and 150 μl of LDL was added and mixed in a tightly sealed glass tube at 24–29°C for 45 min. The reaction was quenched with 3 ml of 6% K_2CO_3. Fatty acid methyl esters were extracted with 300 μl of hexane, transferred to a test tube, and evaporated. The residue was dissolved in 100 μl of decane and transferred to vials for a Hewlett-Packard 7683 injector. Fatty acid methyl esters were separated on a 30 m × 0.25 mm fused silica AT-255 column via 50% cyanopropylphenyl-dimethylpolysiloxan stationary phase (Alltech Associates, Deerfield, IL). Analyses were performed on a Hewlett-Packard 6890 gas chromatograph coupled to a Hewlett-Packard 5973 mass selective detector operated in the electron-impact mode (70 eV) with full-scan monitoring. The elution program consisted of 2 min at 70°C, increase to 180°C at 20°C/min and to 220°C at 3.0°C/min, and hold for 16 min. Injector and detector temperatures were 250°C. Peaks were identified on the basis of retention times and mass spectral analysis of standards (Sigma-Aldrich) from the National Institute of Standards and Technology (standard reference data-

base number 69). For quantification, the peak area of each sample was compared with that of the internal standard.

Thin-layer chromatography of LDL lipids and lipids scavenged by HSA

LDL subfractions (1 mg of protein) were incubated with and without HSA (10 mg) for 60 min at 4°C and separated by ultracentrifugation (d = 1.12 g/ml). The floated LDL and sedimented HSA were collected and extracted in accordance with Folch, Lees, and Sloane Stanley (31), and the dried residue was analyzed by high-performance TLC, as described by White et al. (38), and compared with lipid standards. Lipids were visualized with primulin (Sigma-Aldrich); lipid standards were from Avanti Polar Lipids (Alabaster, AL). The eluting solvents were of HPLC grade. The primulin-stained lipids on the TLC plates were scanned with a Molecular Dynamics Storm imaging system. Subsequently, the lipid bands on the scanned images were quantified using Molecular Dynamics ImageQuant software (version 5.2). All pixels inside the rectangle enclosing each band were integrated; background correction was performed by subtracting the intensity of a duplicate rectangle in a proximal region without visible staining. The calculation of lipid composition was based on integrated values, assuming no lipid-specific differences in relative staining intensity. Lipids associated with LDL protein were applied to each lane in amounts corresponding to equal protein.

NEFA loading of LDL

Assuming molecular weights of 282 and 512,000, respectively, for oleic acid and apoB, oleic acid in ethanol (50 mM) was added to 1–2 mg of LDL at an oleate-to-apoB-100 molar ratio of 125 and incubated for 15 min at 37°C. The final ethanol and oleate concentrations were ≤1% and 0.5 mM, respectively. After exhaustive dialysis against TBS, changes in LDL charge were determined by agarose gel electrophoresis.

Statistical analysis

The significance of trends in LDL properties was determined via one-way ANOVA.

RESULTS

LDL subfractionation according to density

LDL isolated by density gradient ultracentrifugation was collected into seven fractions that were analyzed for charge, composition, and lipid transfer dynamics (**Fig. 1**). The majority of the LDL protein (~85%) was confined to fractions D2 through D5 (Fig. 1A). The remainder appeared in fractions D1, D6, and D7; D7 is the least abundant fraction, comprising only 1.7% of the total protein. An infranatant fraction of lipid-poor material that sediments during ultracentrifugation (data not shown) typically contains approximately half of the amount of protein found in fraction D7. According to the criteria of Berg et al. (39), D5, D6, and D7 are small, dense LDLs (d = 1.048–1.063 g/dl). These subfractions account for ~25% of the total LDL protein.

Analysis of LDL charge

Analysis of the LDL by agarose gel electrophoresis showed fraction-specific differences in particle charge (Fig. 1B); D7 was the most electronegative, followed by two other minor fractions, D1 and D6. In each instance, agarose gel electrophoresis of each LDL subfraction revealed a single broad band. In contrast, anion-exchange chromatography of each LDL subfraction resolved the sample into two major fractions (Fig. 1C), an early-eluting electropositive particle, LDL(+), and a late-eluting electronegative particle, LDL(−). Fractions D2 through D5 contained relatively little (4–13%) LDL(−). However, minor fractions D1, D6, and D7 were rich in LDL(−), 33–85%. In sum, an examination of the agarose gel electrophoresis data shows that the LDL subfractions with the highest electronegativity have the highest content of LDL(−).

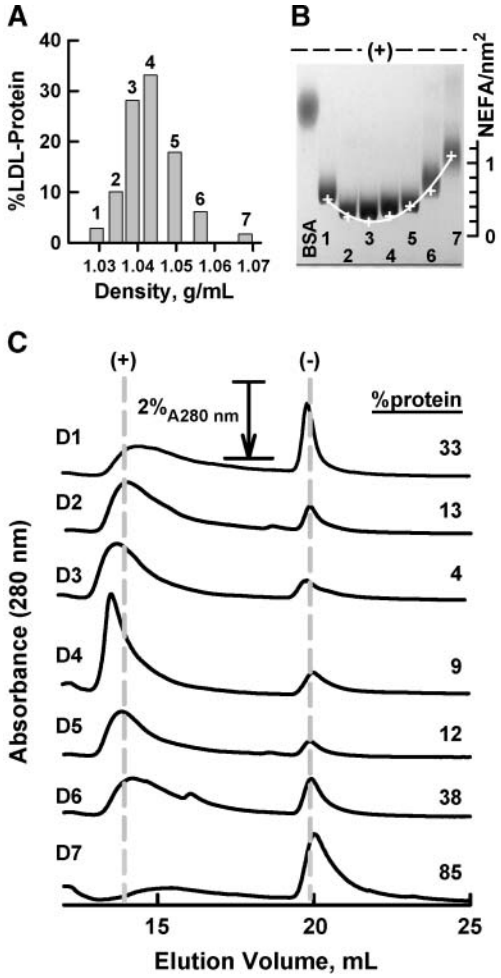

Fig. 1. Characterization of LDL subfractions according to density and charge. A: Densities and relative abundance of seven human LDL subfractions (D1 = 1, etc.) isolated by gradient ultracentrifugation (n = 18); the infranatant contained approximately half the amount of protein that appeared in D7. Error bars represent SEM. B: Relative agarose gel electrophoretic mobility of the D1 through D7 subfractions. The line graph overlay compares the surface densities of NEFA in each subfraction (see Table 1). Samples (5 μg of protein) were loaded into wells at the bottom (cathode) of 0.78% agarose gels and electrophoresed for 90 min at 100 V. At 0.78% agarose, there is no sieving effect; thus, mobility reflects charge. C: Elution of LDL subfractions from a Mono-Q column. Electropositive low density lipoprotein [LDL(+)] and electronegative low density lipoprotein [LDL(−)] are denoted by vertical gray lines. The percentage of total protein in the LDL(−) peak was calculated using the software provided with the instrument.

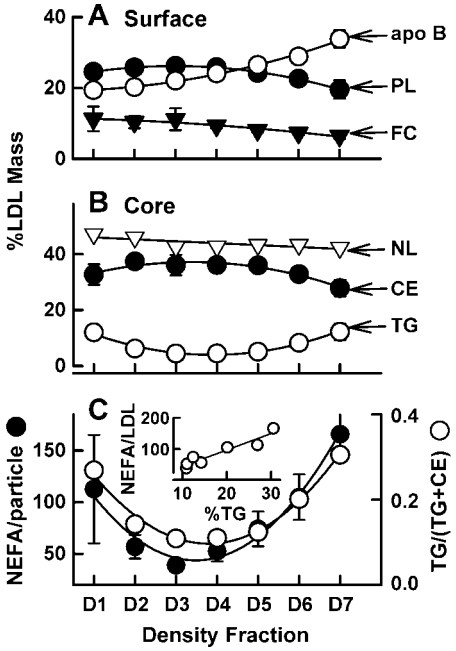

Fig. 2. Compositions of LDL subfractions. A: Surface components. FC, free cholesterol; PL, phospholipid. B: Core lipids. CE, cholesteryl ester; NL, total neutral lipid (CE + TG); TG, triglyceride. Core and surface compositions are expressed as percentage of total LDL weight. C: Percentage of neutral lipid occurring as TG (open circles) and number of NEFA molecules per LDL particle (closed circles), assuming that apolipoprotein B-100 (apoB-100) is the sole protein (512 kDa) and that there is one copy of apoB-100 per LDL particle. The NEFA per particle and percentage neutral lipid as TG were linearly correlated (inset; $r^2 = 0.90$). Data are means ± SEM (n = 9). Error bars represent SEM.

LDL composition

Figure 2 shows the composition of different density subfractions, with respect to surface (A) and core (B) composition and NEFA content (C). As expected, this analysis revealed trends in composition, based on differences in density and size. For example, with D1 through D7, there was a significant increase in protein content with increasing density (20–35%; Fig. 2A) (one- way ANOVA, $P < 0.0001$). PL content decreased slightly with increasing density, and, as expected, FC, which associates mainly with PL, demonstrated a similar pattern (Fig. 2A). Although total neutral lipids [CE + triglyceride (TG)] declined from 45% to 40% (Fig. 2B), the specific contributions of CE and TG varied according to the subfraction. The highest CE and lowest TG contents were observed in the middle fractions, whereas D1 and D7, at opposite ends of the density continuum, had the lowest CE and highest TG contents. Based on LDL composition, known partial specific volumes of the components, and the assumption of one copy of apoB-100 per particle, the calculated diameters ranged from 20.71 nm for D1 to 16.95 nm for D7 (**Table 1**). Using the known densities, we determined that these dimensions correspond to relative particle masses of 100, 95.8, 87.4, 79.9, 72.7, 66.7, and 56.9% for D1 through D7, respectively. The composition of the infranatant (i.e., ~54% protein, ~15% TG, ~4% FC, 14% CE, and 13% PL), which did not correspond to a normal lipoprotein class, is likely a mixture of lipid-free protein, precipitated LDL, HDL, and lipoprotein [a] (Lp[a]). Others have used the LDL fractions of $1.02 < d < 1.05$ g/ml to identify differences between LDL(+) and LDL(−). Although this eliminates the possible confounding effects of Lp[a] that can exist in fractions with greater density, it also excludes the fractions corresponding to D6 and D7 in our study, which are profoundly different from the more electropositive fractions, including those with the highest affinity for $LpPLA_2$. According to ELISA analysis (40), Lp[a] constituted <3% of any LDL subfraction (data not shown).

The NEFA contents of the LDL subfractions were statistically different ($P < 0.015$); regression analyses showed significant linear ($P < 0.036$) and nonlinear ($P < 0.035$) trends, with a decrease and increase in NEFA from D1 to D3 and D3 to D7, respectively (Fig. 2C). The NEFA/apoB-100 molar ratios were highest at the extremes of LDL density: NEFA/apoB-100 = 112, 56, 38, 52, 74, 105, and 166 for D1 through D7, respectively. Calculation of the surface densities of NEFA on LDL demonstrated a similar pattern, except that the NEFA density of D7 was more than twice that of D1 and five times that of D3 (Table 1). Of interest, alterations in NEFA across the density spectrum paralleled changes in electrophoretic mobility and TG

TABLE 1. Properties of LDL subfractions isolated according to density

Fraction	d	D[a]	Mass[b]	ΔG ($LpPLA_2$)[c]	ApoC-III	NEFA/nm^2[d]
	g/ml	*nm*	*kDa*	*kcal*		
D1	1.029	20.71	2,640 (100)	0.00	+	0.083
D2	1.034	20.38	2,530 (95.8)	0.35	+	0.043
D3	1.039	19.74	2,320 (87.4)	0.11	−	0.031
D4	1.043	19.13	2,120 (79.9)	−0.68	−	0.045
D5	1.050	18.50	1,930 (72.7)	−1.44	+	0.069
D6	1.056	17.94	1,770 (66.7)	−2.08	+	0.104
D7	1.068	16.95	1,510 (56.9)	−2.60	+	0.184

ApoC-III, apolipoprotein C-III; $LpPLA_2$, lipoprotein-associated phospholipase A_2.
[a] Diameter calculated from partial specific volumes and compositions.
[b] LDL mass = 100 × 512,000/% protein (mass relative to D1).
[c] $\Delta G = -RT \ln K$, where $K = (LpPLA_2)_{D7}/(LpPLA_2)_{Di}$ and $(LpPLA_2)_{D7}$ and $(LpPLA_2)_{Di}$ are the amounts of $LpPLA_2$ associated with each fraction (i) relative to apoB-100.
[d] Number of NEFA molecules per surface area of a spherical particle given by $A = 4\pi r^2$; a plot of this is overlaid on the agarose gel in Fig. 1B.

TABLE 2. NEFA compositions of LDL subfractions

Fraction	Laurate (C12:0)	Myristate (C14:0)	Palmitate (C16:0)	Palmitoleate (C16:1)	Stearate (C18:0)	Oleate (C18:1)	Linoleate (C18:2)	Arachidonate (C20:4)	Unsaturated/ Saturated
D1	0.5 ± 0.09	1.6 ± 0.01	22.9 ± 1.2	1.5 ± 0.10	12.6 ± 0.76	18.0 ± 0.37	**38.6 ±2.1**	4.4 ± 0.42	1.66
D2	0.1 ± 0.02	0.8 ± 0.14	19.4 ± 1.9	0.8 ± 0.14	9.1 ± 0.11	18.4 ± 0.90	45.7 ± 3.2	5.6 ± 0.40	2.40
D3	0.1 ± 0.02	0.7 ± 0.13	17.3 ± 0.9	0.7 ± 0.09	9.4 ± 0.68	18.1 ± 1.4	47.2 ± 1.9	6.5 ± 0.47	2.64
D4	0.1 ± 0.02	0.8 ± 0.13	17.0 ± 1.4	0.7 ± 0.08	9.5 ± 0.29	18.2 ± 0.73	47.1 ± 2.7	6.5 ± 0.68	2.65
D5	0.2 ± 0.03	0.9 ± 0.14	18.7 ± 1.3	0.8 ± 0.09	9.0 ± 0.11	17.5 ± 0.82	46.1 ± 2.9	6.8 ± 0.71	2.47
D6	0.5 ± 0.11	1.6 ± 0.21	21.6 ± 1.5	1.3 ± 0.20	10.9 ± 0.22	16.3 ± 1.0	41.0 ± 3.1	6.8 ± 0.32	1.89
D7	**1.1 ± 0.24**	**3.0 ± 0.66**	**27.5 ± 1.5**	**2.9 ± 0.70**	**17.3 ± 0.88**	**13.3 ± 0.14**	**29.5 ± 2.7**	5.5 ± 0.27	1.05

NEFA composition values are given in percentage (n = 3). Correlation coefficients that are statistically significant for trends ($P < 0.05$) are depicted in boldface type.

content, with which it was positively correlated (Fig. 2C and inset; $r^2 = 0.90$). An overlay of the surface density of NEFA on LDL (molecules/nm^2) on the agarose gel (Fig. 1B) shows that NEFA content accounted for much of the variation in LDL charge.

There were also differences in NEFA acyl chain molecular species composition among the LDL subfractions. For some subfractions, the abundance of NEFA emulates that of total NEFA, whereas others exhibit the opposite distribution (**Table 2**). The most abundant fatty acid in all fractions is linoleate; this NEFA is more abundant in D2 through D6 than in D1 and D7. Oleate is less abundant in D7 than in D1 through D6. The remainder of the fatty acids (i.e., laurate, myristate, palmitate, palmitoleate, and stearate) exhibit a NEFA distribution profile similar to that of total NEFA; they are more abundant in D1 and D7 than in the middle fractions. Arachidonate is similar in all subfractions. The ratios of unsaturated to saturated fatty acids in the major subfractions D3 (2.63) and D4 (2.64) were greater than those for D1 (1.66) and especially D7 (1.05).

TLC analysis of LDL lipid dynamics

The differences in NEFA content among the various LDL fractions suggested that this might be the source of electronegative charge and that transferring NEFA to its major plasma carrier, HSA, could convert LDL(−) to its electropositive counterpart. This hypothesis was tested using the LDL of four human subjects. The pooled lipid compositions (D3 + D4 and D6 + D7) of subjects A, B, C, and D were analyzed by TLC before and after incubation with albumin. TLC disclosed all of the major lipids found by chemical analysis (**Fig. 3A**). In addition, TLC showed that the more dense fractions from subjects A through D contained more lysophosphatidylcholine (lyso PC; ~3×) than those found in less dense fractions from subjects A through C. The incubation of LDL (D3 + D4) and LDL (D6 + D7) with HSA alters the TLC pattern (Fig. 3A, B). In each case, incubation with HSA (60 min at 4°C) reduced the amount of NEFA and lyso PC, the other major monoacyl lipid carried by albumin. TLC analysis of the HSA extracts after incubation with the LDL fractions showed the transfer of both NEFA and lyso PC to HSA (Fig. 3B). This transfer was particularly profound for D6 + D7 from subjects A through D. Lyso PC was reduced by an average of 29% in the D3 + D4 fractions and by 42% in the D6 + D7 fractions. No lipids were found in the organic extracts of the HSA used for scavenging (Fig. 3, penultimate lanes). LDL electronegativity, as assessed by agarose gel electrophoresis, was reduced by this incubation (data not shown).

In addition to NEFA and lyso PC, small amounts of all lipid classes were found among the HSA-scavenged

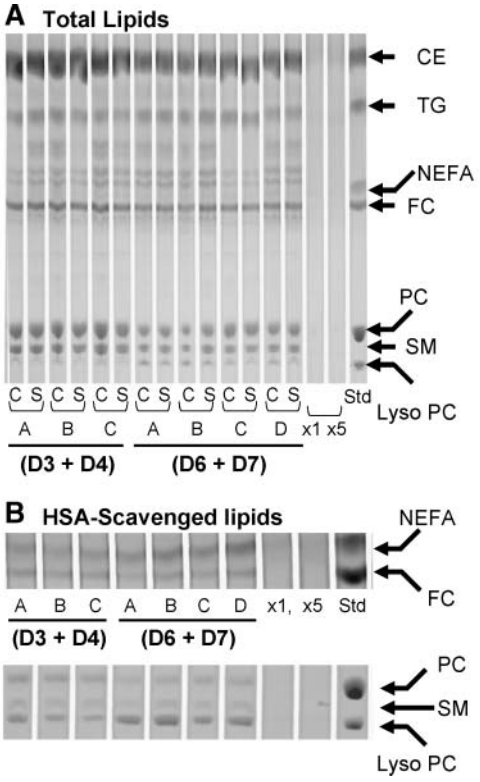

Fig. 3. TLC of lipid extracts from LDL subfractions and lipids scavenged by human serum albumin (HSA). Subfractions D3 + D4 from donors A, B, and C were pooled and analyzed by TLC before (C, control) and after scavenging with HSA (S, scavenged). Subfractions D6 + D7 from donors A through D were similarly analyzed; D is a donor for whom no D3 + D4 was analyzed. A: TLC analysis of total lipids. B: TLC of HSA-scavenged lipids. Detail at bottom shows regions of interest that reveal the monoacyl lipids, NEFA, and lysophosphatidylcholine (Lyso PC). The last lane contains standards (Std); the lanes to the left of the standards contain lipid extracts of 1× and 5× the amount of HSA that was used to scavenge lipids from LDL. The same amount of LDL protein was extracted for each test lane. SM, sphingomyelin.

lipids (Fig. 3B). This may have been solely attributable to the sedimentation of traces of total LDL during the d = 1.12 g/ml ultracentrifugation step; traces of LDL attached to the walls of the centrifuge tubes may have been captured along with the HSA-associated lipids. However, relative to NEFA and lyso PC, the amounts of other lipids were small.

Transfer of LDL electronegativity to HDL

Given the lipophilic and cardioprotective nature of HDL, we tested whether the electronegative charge of LDL(−) could also be transferred to HDL. Incubation with increasing amounts of HDL was associated with a dose-dependent decrease in the electronegativity of D7, with a parallel increase in HDL electronegativity (**Fig. 4A**, lanes 1 and 2 vs. lanes 3–6). However, even at the highest doses of HDL, the charge reduction did not reach that of D3 (Fig. 4A, cf. lanes 6 and 8). The addition of HDL to D3, even at high doses, had only a small effect on its electrophoretic mobility (Fig. 4B, lanes 1–3). After the addition of oleate, the electrophoretic behavior of D3 emulated that of LDL(−) (Fig. 4B, lane 4), an effect that was reversed in a dose-dependent manner by the addition of HDL (Fig. 4B, lanes 5–8). In contrast, lyso PC treatment of LDL(+) had no effect on electrophoretic mobility (data not shown). Reconstituted HDL, composed of POPC and apoA-I, also scavenges the electronegative charge; however, apoA-I alone was ineffective. HDL does not alter the electronegativity of acetylated LDL and only slightly reduces that of copper-oxidized LDL (data not shown). This suggests that the basis of electronegativity in these forms of modified LDL is not NEFA.

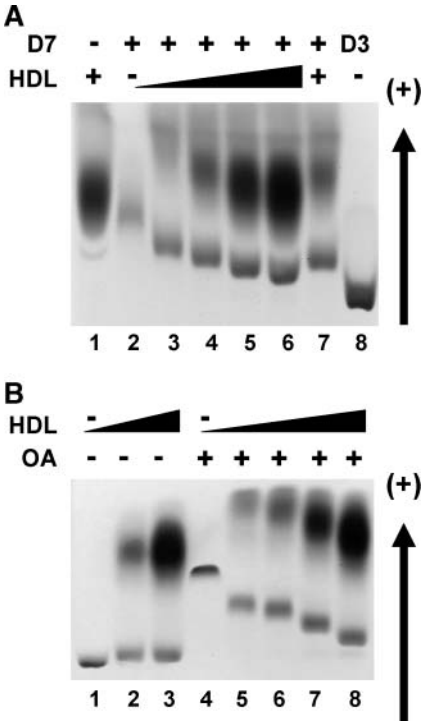

Fig. 4. Charge transfer from LDL to HDL revealed by agarose gel electrophoresis. A: Lane 1, HDL (50 μg of protein); lane 2, D7 (10 μg of protein); lanes 3–6, D7 (7.5 μg of protein) plus HDL (12.5, 20, 50, and 75 μg of protein, respectively); lane 7, repeat of lane 3 demonstrating gel and electric field uniformity; lane 8, D3. B: HDL removal of charge from D3 (lanes 1–3) and D3 loaded with oleate (OA; lanes 4–8). All lanes contain D3 (10 μg). Lane 1, D3 only; lanes 2 and 3, D3 + HDL (20 and 80 μg, respectively); lane 4, oleate-treated D3; lanes 5–8, HDL (10, 20, 40, and 80 μg of protein, respectively) + oleate-treated D3. Oleate/apoB-100 (m/m) = 130, assuming molecular weights of 283 and 512,000.

Distribution of $LpPLA_2$ and oxidized LDL according to density

Both Western blot analysis (**Fig. 5A**) and quantitative ELISA (Fig. 5B) showed that $LpPLA_2$ had a profound preference (i.e., highest free energy) for association with the densest LDL fractions (Table 1). The $LpPLA_2$/apoB molar ratio was 1:100 and 1:10,000 for D7 and D2, respectively, showing that even in the D7 subfraction, only 1% of the LDL particles contained $LpPLA_2$; most LDL particles did not contain $LpPLA_2$. The $LpPLA_2$ content of the infranatant was one-third that of D7. In contrast, the oxidized LDL content of each fraction, measured as apoB-100 oxidation by ELISA, was similar (Fig. 5C; $r^2 = 0.038$).

Distribution of $LpPLA_2$ according to density and charge

To better localize $LpPLA_2$ to specific LDL fractions, D1 and D6 were fractionated by ion-exchange chromatography (as in Fig. 1C) into two fractions for LDL(+), leading

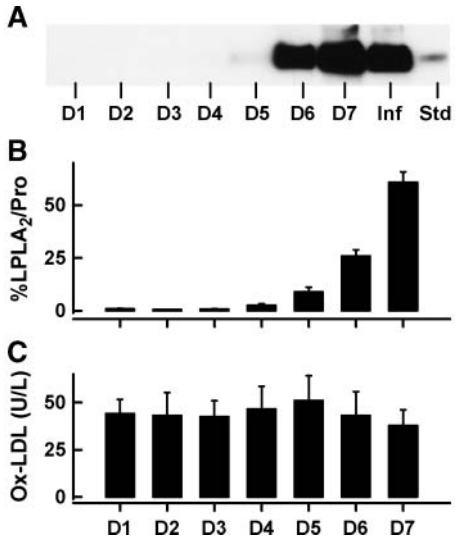

Fig. 5. Lipoprotein-associated phospholipase A_2 ($LpPLA_2$) and oxidized LDL (Ox-LDL) contents of LDL subfractions. A: Representative $LpPLA_2$ Western blot. LDL proteins (10 μg) were resolved by SDS-PAGE (4–15%) and transferred to polyvinylidene difluoride membranes; relative amounts of $LpPLA_2$ were determined by chemiluminescence with an antibody to $LpPLA_2$. Inf, infranatant fraction; Std, $LpPLA_2$ standard. B: Association of $LpPLA_2$ with LDL subfractions according to ELISA (n = 12). $LpPLA_2$ blot data band intensity was determined by ImageQuant densitometry. C: Oxidized LDL levels according to an ELISA (n = 4) that detects oxidized apoB-100. Oxidized LDL levels of LDL subfractions were not statistically different. Data are means ± SEM. Error bars represent SEM.

(L) and trailing (T) fractions, as well as LDL(−). These fractions were analyzed for charge by agarose electrophoresis (**Fig. 6A**) and for $LpPLA_2$ by ELISA (Fig. 6B). Our data show the highest and lowest concentrations of $LpPLA_2$ in the dense LDL(−) and the buoyant LDL(+), respectively. Within the D6 and D1 subfractions, differences in the association of $LpPLA_2$ with LDL(+) L and LDL(+) T were not significant, whereas differences between D1 and D6 LDL(−) were significant (6- to 12-fold). The $LpPLA_2$ content of D6 was greater than that of the corresponding fractions of D1: 170, 330, and 370% for LDL(+) L, LDL(+) T, and LDL(−), respectively. Thus, a component of $LpPLA_2$ binding is associated with density, but the association with electronegativity is stronger.

ApoC-III distribution

Given the association between TG and apoC-III, Western blot analysis was used to determine the distribution of apoC-III among LDL subfractions derived from five subjects. In all instances, apoC-III appeared in D1 or D2 and D6 and D7, but not in D3 and D4, which contain >60% of the LDL protein (**Fig. 7**). The infranatant fraction also contained some apoC-III, which may have desorbed from LDL during centrifugation. Thus, unlike $LpPLA_2$, apoC-III content is higher in LDL subfractions with higher TG, irrespective of density. Of note is the individual variability in relative amounts of apoC-III in the low (D1) and high (D6 and D7) density fractions.

We compared paired plasma and LDL samples processed with and without the addition of inhibitors of lipolysis (tetrahydrolipstatin) and oxidation (butylated hydroxytoluene) and found no significant differences in the density-dependent differences in mobility in agarose gel electrophoresis, NEFA concentration, and $LpPLA_2$ activity (data not shown). These observations demonstrate that the observed density-dependent differences are not attributable to artifactual in vitro lipolysis or oxidation.

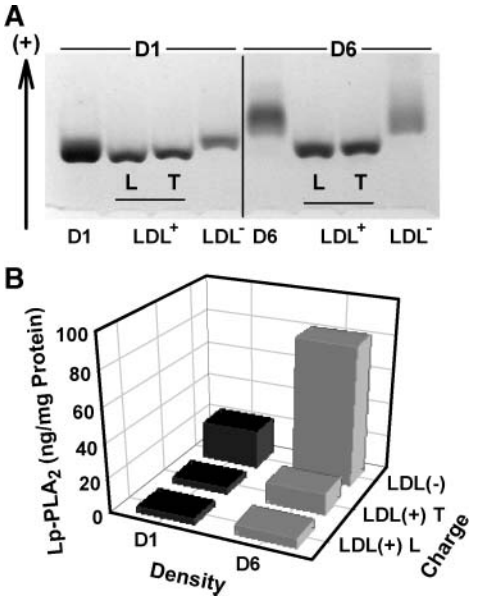

Fig. 6. Distribution of $LpPLA_2$ mass according to LDL charge and density. Fractions D1 and D6 were fractionated by Mono-Q ion-exchange chromatography. The leading (L) and trailing (T) edges of the LDL(+) and a single LDL(−) peak were collected, concentrated, separated by agarose electrophoresis, and analyzed for $LpPLA_2$ mass by ELISA. A: Agarose gel electrophoresis. B: Distribution of $LpPLA_2$ according to density and relative charge.

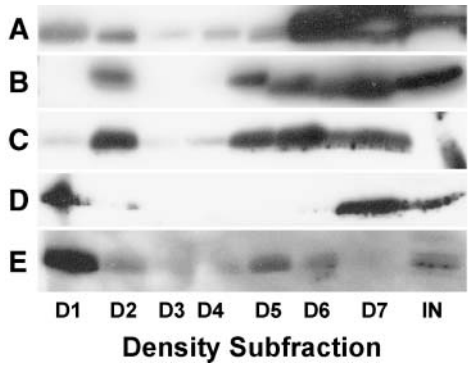

Fig. 7. Distribution of apoC-III among LDL subfractions D1 through D7 and infranatant (Inf) from five donors (A–E). LDL subfractions (10 μg) were electrophoresed by SDS-PAGE (15%) and transferred and blotted with an antibody against apoC-III. The apoC-III bands were visualized by enhanced chemiluminescence.

DISCUSSION

NEFA and LDL electronegativity

The biology and chemistry of LDL(−) have been topics of interest since the report of Avogaro, Bittolo-Bon, and Cazzolato (9) in 1988; that early work has been reviewed and richly expanded by Sánchez-Quesada, Benitez, and Ordonez-Llanos (41), who recently summarized the current state of knowledge regarding LDL(−). Through density gradient ultracentrifugation and sequential flotation, we separated LDL from normolipemic human plasma into seven subfractions and characterized each, according to *1*) charge, via agarose gel electrophoresis and ion-exchange chromatography; *2*) chemical composition, by lipid class; and *3*) fatty acid molecular species composition of associated NEFA, *4*) $LpPLA_2$, *5*) apoC-III, *6*) oxidized LDL, and *7*) Lp[a]. In addition, we tested and confirmed that HSA and HDL alter the chemical and electrophoretic properties of LDL(−) by scavenging their associated NEFAs.

Both ion-exchange chromatography and agarose gel electrophoresis revealed differences in charge across the density range of LDL. Although only one broadly distributed species is seen in the electrophoretic patterns, two species are observed via ion-exchange chromatography. The relative mobility observed by electrophoresis correlates well with the abundance of the most electronegative fraction observed by chromatography; this has been a consistent observation of nearly all who have studied LDL(−). The variation in results by ion-exchange chromatography and agarose gel electrophoresis may be attributable in part to the exchangeable character of NEFA, which imbues LDL with a major portion of its electronegativity, as well as

to differences in the way the two techniques separate molecules and/or particles.

Although subfractionation of LDL according to density is independent of charge, this method nevertheless yielded seven subfractions that exhibited charge differences as assessed by agarose gel electrophoresis and ion-exchange chromatography. Charge differences in lipoproteins have been attributed to apolipoprotein composition and conformation and NEFA content (41). La Belle, Blanche, and Krauss (42) compared LDL charge heterogeneity in patients with LDL pattern A and those having pattern B and concluded that the greater electronegativity of dense LDL is attributable to greater charge density that is related to smaller surface area and not to increased valence, as is the case for more buoyant LDL. Our data suggest that the differences in charge density are the result of differences in NEFA density, which tracks very well with electrophoretic mobility (Fig. 1B); this conclusion is supported by NEFA add-back and removal experiments showing that NEFA content affects electronegativity in a predictable way.

Thus, our data provide strong support for a model of LDL in which NEFA content is the major, if not the sole, determinant of LDL electronegativity. The addition of the physiologically abundant NEFA, oleic acid, increased the electronegativity of LDL. Although particle size can determine LDL electrophoretic mobility, under our conditions (0.7% agarose), the sieving effect is minimal and the electrophoretic mobility of particles on the agarose gels is determined by surface charge density. Thus, we believe that the most convincing evidence that the electrophoretic mobility of LDL is attributable mainly to NEFA content is provided by the correlation of charge with the surface density of NEFA (Fig. 1B). From the data of Braschi et al. (43) and Phillips et al. (44), we calculated NEFA/apoB molar ratios of 50 and 109, respectively, for LDL(+) and LDL(−); these ratios are very similar to our findings (Fig. 2C). Although our ratios are approximately three times higher than those of Benítez et al. (45), who found a less dense electronegative fraction in LDL from hypertriglyceridemic and familial hypercholesterolemic patients but not normolipidemic subjects, these differences are likely a function of methodology. Benítez et al. (45) incubated LDL with a NEFA mixture in the presence of lipoprotein-deficient serum, which contains albumin; we used oleate without albumin. Albumin likely removed some of the LDL-NEFA, resulting in the lower ratio reported in that study. Alternatively, the preferential association of some NEFA species with different LDL subfractions (Table 2) could also yield different ratios.

The distribution of NEFA among LDL subfractions is assumed to be at equilibrium because the half-times for NEFA exchange among lipoproteins are on the order of 20 ms (46). Moreover, we observed a rapid transfer of NEFA from LDL to HDL and HSA (Figs. 3, 4). Thus, the density-specific distribution of NEFA species is thermodynamically controlled so that some fractions, both electropositive and electronegative, have properties that enhance the binding of some NEFAs over others. We believe that this property is associated with another prominent difference in LDL composition that correlates with LDL-NEFA: LDL-TG. Although LDL-TG and LDL-NEFA are associated (Fig. 2C), it is likely that the TG content controls NEFA content, rather than vice versa; unlike NEFA, TG content is not exchangeable in the absence of plasma transfer proteins, which give rise to its increased concentration in a stationary state. Therefore, we propose that NEFA, particularly saturated NEFA, preferentially associates with D1 and D7 because of their higher TG content. According to current models, the core of LDL is composed of CE, TG, and FC. However, measurable amounts of neutral lipid can be solubilized by PL, and studies of mixed emulsions of TG, CE, and PL have shown that 10 times or more TG than CE partitions into the PL phase (47). These findings suggest that the mixed monolayer of PL and TG on the surface of LDL could increase the affinity of NEFA for TG-rich LDL. Nevertheless, the basis for the preferential association of specific fatty acid species with TG-rich LDL over TG-poor LDL remains unclear and is currently under investigation. The role of NEFA composition on LDL subfraction atherogenicity also remains to be determined.

$LpPLA_2$ association with dense LDL(−)

Our data (Fig. 5) confirm the report of McCall et al. (48), who quantified $LpPLA_2$ association with subfractions isolated in density gradients, as in our study, as well as by size-exclusion chromatography. They also observed a nondissociable pool of $LpPLA_2$ that is greatly enriched in the small, dense LDL subfractions. $LpPLA_2$ is highly specific to fractions that are dense, electronegative, and rich in TG, apoC-III, and NEFA, particularly saturated NEFA. Furthermore, its preferential association with D7 is not attributable to electronegativity, TG, or NEFA content because D1, which is also electronegative and contains relatively

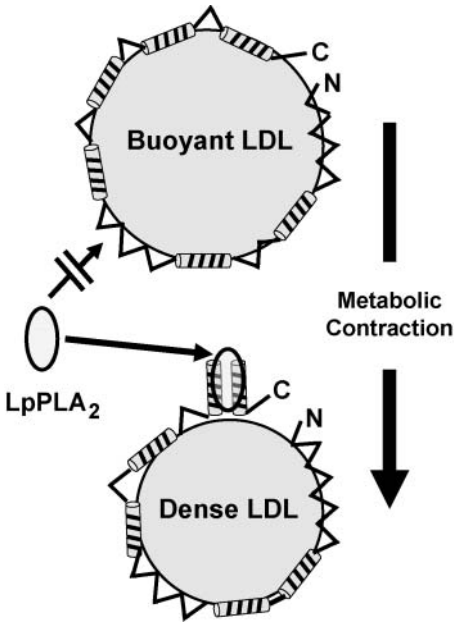

Fig. 8. Model for the association of $LpPLA_2$ with small, dense LDL(−).

high amounts of both lipids, contains very little $LpPLA_2$. Relative to D1 through D3, the free energy of association of $LpPLA_2$ with D7 is more exergonic, by ~2.5 kcal. This difference could result from the association of $LpPLA_2$ with regions of apoB-100 that are not accessible or exposed in the larger, more electropositive fractions. Clues to their identity emerge from a proposed model of LDL and recent tests of that model. Segrest et al. (49) proposed a model of apoB-100 as a protein with five superdomains composed of three amphipathic α-helical (AαH) domains alternating with two amphipathic β-strand (AβS) domains. The distinctive roles of these domains were elucidated in a recent study of surface pressure effects on various peptides of apoB-100. Wang, Walsh, and Small (50) showed that binding of apoB to a model of the TG/water interface decreases interfacial tension and free energy. According to attendant changes in interfacial tension, compression of the apoB-100 surface causes a fraction of the protein to desorb into the aqueous phase while still tethered to the polypeptide chain. Given their structural homology with the exchangeable apolipoproteins, which readily desorb between lipid surfaces and water, the authors suggest that in response to monolayer compression, some of the AαH domains desorb from the lipid surface. Conversely, AβS domains anchor apoB to the surface and are its nonexchangeable (i.e., nondesorbing) motif. The conformational changes induced by surface pressure, and perhaps composition, may be critical to $LpPLA_2$ binding. Through several metabolic processes, including lipolysis and neutral lipid transfer, LDL contracts to a smaller species. $LpPLA_2$ binds to the C-terminal region of apoB-100 (51). We propose that $LpPLA_2$ binds to apoB-100 via one or more C-terminal AαH domains that are desorbed by increased surface pressure in response to the metabolic contraction of LDL core lipids (**Fig. 8**).

Substantial amounts of NEFA are associated with the D1 and D7 LDL fractions, and these levels are expected to be even higher after aerobic exercise or fat consumption, both of which increase plasma NEFA. High LDL-NEFA levels are also expected in pathological states that are associated with increased NEFA, including severe diabetic ketoacidosis, hyperlipidemia, and hypoalbuminemia. NEFA has a higher affinity for phospholipids than for HSA (46, 52); thus, even in the presence of high physiological concentrations of albumin, measurable amounts are associated with plasma lipoproteins (46, 52). Although the transfer of NEFA to HDL and HSA is likely a detoxification mechanism, the amount transferred to HDL is expected to be small because the albumin pool is so much larger than that of HDL. Thus, the major effect of increased plasma NEFA may be to increase the NEFA content of specific LDL fractions, thereby increasing the association with specific proteins through increased negative charge.

This work was supported by grants-in-aid from the National Institutes of Health (Grants HL-30914 and HL-56865 to H.J.P.) and the American Heart Association, Texas Affiliate (Grant 0465060Y to R.C.H.).

REFERENCES

1. Navab, M., J. A. Berliner, A. D. Watson, S. Y. Hama, M. C. Territo, A. J. Lusis, D. M. Shih, B. J. Van Lenten, J. S. Frank, L. L. Demer, et al. 1996. The yin and yang of oxidation in the development of the fatty streak. *Arterioscler. Thromb. Vasc. Biol.* **16:** 831–842.
2. Kovanen, P. T., and M. O. Pentikäinen. 2003. Circulating lipoproteins as proinflammatory and anti-inflammatory particles in atherogenesis. *Curr. Opin. Lipidol.* **14:** 411–419.
3. Holvoet, P., J. Vanhaecke, J. Janssens, F. Van de Werf, and D. Collen. 1998. Oxidized LDL and malondialdehyde-modified LDL in patients with acute coronary syndromes and stable coronary artery disease. *Circulation.* **98:** 1487–1494.
4. Ehara, S., M. Ueda, T. Nakuro, K. Haze, A. Itoh, M. Otsuka, R. Komatsu, T. Matsuo, H. Itabe, T. Takano, et al. 2001. Elevated levels of oxidized low density lipoprotein show a positive relationship with the severity of acute coronary syndromes. *Circulation.* **103:** 1955–1960.
5. Nishi, K., H. Itabe, M. Uno, K. T. Kitazato, H. Horiguchi, K. Shinno, and S. Nagahiro. 2002. Oxidized LDL in carotid plaques and plasma associates with plaque instability. *Arterioscler. Thromb. Vasc. Biol.* **22:** 1649–1654.
6. Schuh, J., G. F. Fairclough, and R. H. Haschemeyer. 1978. Oxygen-mediated heterogeneity of apo-low-density lipoprotein. *Proc. Natl. Acad. Sci. USA.* **75:** 3173–3177.
7. Kim, H. J., and I. V. Kurup. 1982. Nonenzymatic glycosylation of human low density lipoprotein: evidence for in vivo and in vitro glucosylation. *Metabolism.* **31:** 348–352.
8. Orekhov, A. N., V. V. Tertov, D. N. Mukhin, and I. A. Mikhailenko. 1989. Modification of low density lipoprotein by desialylation causes lipid accumulation in cultured cells: discovery of desialyated lipoprotein with altered cellular metabolism in the blood of atherosclerotic patients. *Biochem. Biophys. Res. Commun.* **162:** 206–211.
9. Avogaro, P., G. Bittolo-Bon, and G. Cazzolato. 1988. Presence of a modified low density lipoprotein in humans. *Arteriosclerosis.* **8:** 79–87.
10. Bittolo-Bon, G., G. Cazzolato, and P. Avogaro. 1994. Probucol protects low-density lipoproteins from in vitro and vivo oxidation. *Pharmacol. Res.* **29:** 337–344.
11. Vedie, B., X. Jeunemaitre, J. L. Mégnien, I. Myara, H. Trebeden, A. Simon, and N. Moatti. 1998. Charge heterogeneity of LDL in asymptomatic hypercholesterolemic men is related to lipid parameters and variations in the apo B and CIII genes. *Arterioscler. Thromb. Vasc. Biol.* **18:** 1780–1789.
12. Sánchez-Quesada, J. L., C. Otal-Entraigas, M. Franco, O. Jorba, F. Gonzalez-Sastre, F. Blanco-Vaca, and J. Ordonez-Llanos. 1999. Effect of simvastatin treatment on the electronegative low-density lipoprotein present in patients with familial hypercholesterolemia. *Am. J. Cardiol.* **84:** 655–659.
13. Sánchez-Quesada, J. L., S. Benítez, C. Otal, M. Franco, F. Blanco-Vaca, and J. Ordonez-Llanos. 2002. Density distribution of electronegative LDL (LDL(−)) in normolipemic and hyperlipemic subjects. *J. Lipid Res.* **43:** 699–705.
14. Sánchez-Quesada, J. L., A. Pérez, A. Caixàs, J. Ordonmez-Llanos, G. Carreras, A. Payes, F. Gonzalez-Sastre, and A. de Leiva. 1996. Electronegative low-density lipoprotein subform is increased in patients with short-duration IDDM and is closely related to glycaemic control. *Diabetologia.* **39:** 1469–1476.
15. Sánchez-Quesada, J. L., A. Pérez, A. Caixàs, M. Rigla, A. Payes, S. Benitez, and J. Ordonez-Llanos. 2001. Effect of glycemic optimization on electronegative low-density lipoprotein in diabetes: relation to nonenzymatic glycosylation and oxidative modification. *J. Clin. Endocrinol. Metab.* **86:** 3243–3249.
16. Moro, E., C. Zambón, S. Pianetti, G. Cazzolato, M. Pais, and G. Bittolo Bon. 1998. Electronegative low density lipoprotein subform is increased in type 2 (non-insulin-dependent) microalbuminuric patients and is closely associated with LDL susceptibility to oxidation. *Acta. Diabetol.* **35:** 161–164.
17. Moro, E., P. Alessandrini, C. Zambón, S. Pianetti, M. Pais, G. Cazzolato, and G. B. Bon. 1999. Is glycation of low density lipoproteins in patients with type 2 diabetes mellitus an LDL preoxidative condition? *Diabet. Med.* **16:** 663–669.
18. Tomasik, A., W. Jache, B. Skrzep-Poloczek, E. Widera-Romuk, J. Wodniecki, and C. Wojciechowska. 2003. Circulating electronegatively-charged low-density lipoprotein in patients with angiographically documented coronary artery disease. *Scand. J. Clin. Lab. Med.* **63:** 259–266.

19. Cazzolato, G., P. Avogaro, and G. Bittolo-Bon. 1991. Characterization of a more electronegatively-charged LDL subfraction by ion exchange HPLC. *Free Radic. Biol. Med.* **11:** 247–253.
20. Avogaro, P., G. Cazzolatto, and G. Bittolo-Bon. 1991. Some questions concerning a small, more electronegative LDL circulating in human plasma. *Atherosclerosis.* **91:** 163–171.
21. Hodis, H. N., D. M. Kramsch, P. Avogaro, G. Bittolo-Bon, G. Cazzolato, J. Hwang, H. Peterson, and A. Sevanian. 1994. Biochemical and cytotoxic characteristics of an in vivo circulating oxidized low-density lipoprotein (electronegative LDL). *J. Lipid Res.* **35:** 669–677.
22. Sevanian, A., J. Hwang, H. Hodis, G. Cazzolato, P. Avogaro, and G. Bittolo-Bon. 1996. Contribution of an in vivo oxidized LDL to LDL oxidation and its association with dense LDL subpopulations. *Arterioscler. Thromb. Vasc. Biol.* **16:** 784–793.
23. Shimano, H., N. Yamada, S. Ishibashi, H. Mokuno, N. Mori, T. Gotoda, K. Harada, Y. Akanuma, T. Murase, Y. Yazaki, et al. 1991. Oxidation-labile subfraction of human plasma low-density lipoprotein isolated by ion-exchange chromatography. *J. Lipid Res.* **32:** 763–773.
24. Chappey, B., I. Myara, M. O. Benoit, C. Maziere, J. C. Maziere, and N. Moatti. 1995. Characteristics of ten charge-differing subfractions isolated from human native low-density lipoprotein (LDL). No evidence of peroxidative modifications. *Biochim. Biophys. Acta.* **1259:** 261–270.
25. Demuth, K., I. Myara, B. Chappey, B. Vedie, M. A. Pech-Amsellem, M. E. Haberland, and N. Moatti. 1996. A cytotoxic electronegative LDL subfraction is present in human plasma. *Arterioscler. Thromb. Vasc. Biol.* **16:** 773–783.
26. Nyyssönen, K., J. Kaikkonen, and J. T. Salonen. 1996. Characterization and determinants of an electronegatively-charged low-density lipoprotein in human plasma. *Scand. J. Clin. Lab. Invest.* **56:** 681–689.
27. de Castellarnau, C., J. L. Sánchez-Quesada, S. Benítez, R. Rosa, L. Caveda, L. Vila, and J. Ordonez-Llanos. 2000. Electronegative LDL from normolipemic subjects induces IL-8 and monocyte chemotactic protein secretion by human endothelial cells. *Arterioscler. Thromb. Vasc. Biol.* **20:** 2281–2287.
28. Sánchez-Quesada, J. L., M. Camacho, R. Antón, S. Benitez, L. Vila, and J. Ordonez-Llanos. 2003. Electronegative LDL of FH subjects. Chemical characterization and induction of chemokine release from human endothelial cells. *Atherosclerosis.* **166:** 261–270.
29. Schumaker, V. N., and D. L. Puppione. 1986. Sequential flotation ultracentrifugation. *Methods Enzymol.* **128:** 155–170.
30. Yang, C. Y., J. L. Raya, H. H. Chen, C. H. Chen, Y. Abe, H. J. Pownall, A. A. Taylor, and C. V. Smith. 2003. Isolation, characterization, and functional assessment of oxidatively modified subfractions of circulating low-density lipoproteins. *Arterioscler. Thromb. Vasc. Biol.* **23:** 1083–1090.
31. Folch, J., M. Lees, and G. H. Sloane Stanley. 1957. A simple method for the isolation and purification of total lipids from animal tissues. *J. Biol. Chem.* **226:** 497–509.
32. Hoogeveen, R. C., and C. M. Ballantyne. 2005. PLAC test for identification of individuals at increased risk for coronary heart disease. *Expert Rev. Mol. Diagn.* **5:** 9–14.
33. Lowry, O. H., N. J. Rosebrough, A. L. Farr, and R. J. Randall. 1951. Protein measurement with the Folin phenol reagent. *J. Biol. Chem.* **193:** 265–275.
34. Holvoet, P., E. Macy, M. Landeloos, D. Jones, J. S. Nancy, F. Van de Werf, and R. P. Tracy. 2006. Analytical performance and diagnostic accuracy of immunometric assays for the measurement of circulating oxidized LDL. *Clin. Chem.* **52:** 760–764.
35. Sherman, M. B., E. V. Orlova, G. L. Decker, W. Chiu, and H. J. Pownall. 2003. Structure of triglyceride-rich human low-density lipoproteins according to cryoelectron microscopy. *Biochemistry.* **42:** 14988–14993.
36. Tardieu, A., L. Mateu, C. Sardet, B. Weiss, V. Luzzati, L. Aggerbeck, and A. M. Scanu. 1976. Structure of human serum lipoproteins in solution. II. Small-angle x-ray scattering study of HDL3 and LDL. *J. Mol. Biol.* **105:** 459–460.
37. Lepage, G., and C. C. Roy. 1988. Specific methylation of plasma nonesterified fatty acids in one-step reaction. *J. Lipid Res.* **29:** 227–235.
38. White, T., S. Bursten, D. Federighi, R. A. Lewis, and E. Nudelman. 1998. High-resolution separation and quantification of neutral lipid and phospholipid species in mammalian cells and sera by multi-one-dimensional thin-layer chromatography. *Anal. Biochem.* **258:** 109–117.
39. Berg, G., M. L. Muzzio, R. Wikinski, and L. Schreier. 2004. A new approach to the quantitative measurement of dense LDL subfractions. *Nutr. Metab. Cardiovasc. Dis.* **14:** 73–80.
40. Gaubatz, J. W., G. L. Cushing, and J. D. Morrisett. 1986. Quantitation, isolation, and characterization of human lipoprotein (a). *Methods Enzymol.* **129:** 167–186.
41. Sánchez-Quesada, J. L., S. Benitez, and J. Ordonez-Llanos. 2004. Electronegative low-density lipoprotein. *Curr. Opin. Lipidol.* **15:** 329–335.
42. La Belle, M., P. J. Blanche, and R. M. Krauss. 1997. Charge properties of low density lipoprotein subclasses. *J. Lipid Res.* **38:** 690–700.
43. Braschi, S., L. Lagrost, E. Florentin, C. Martin, A. Athias, P. Gambert, M. Krempf, C. Lallemant, and B. Jacotot. 1996. Increased cholesteryl ester transfer activity in plasma from analbuminemic patients. *Arterioscler. Thromb. Vasc. Biol.* **16:** 441–449.
44. Phillips, C., D. Owens, P. Collins, and G. H. Tomkin. 2005. Low density lipoprotein non-esterified fatty acids and lipoprotein lipase in diabetes. *Atherosclerosis.* **181:** 109–114.
45. Benítez, S., V. Villegas, C. Bancells, O. Jorba, F. Gonzalez-Sastre, J. Ordonez-Llanos, and J. L. Sanchez-Quesada. 2004. Impaired binding affinity of electronegative low-density lipoprotein (LDL) to the LDL receptor is related to nonesterified fatty acids and lysophosphatidylcholine content. *Biochemistry.* **43:** 15863–15872.
46. Massey, J. B., D. H. Bick, and H. J. Pownall. 1997. Spontaneous transfer of monoacyl amphiphiles between lipid and protein surfaces. *Biophys. J.* **72:** 1732–1743.
47. Miller, K. W., and D. M. Small. 1983. Triolein-cholesteryl oleate-cholesterol-lecithin emulsions: structural models of triglyceride-rich lipoproteins. *Biochemistry.* **22:** 443–451.
48. McCall, M. R., M. La Belle, T. M. Forte, R. M. Krauss, Y. Takanami, and D. L. Tribble. 1999. Dissociable and nondissociable forms of platelet-activating factor acetylhydrolase in human plasma LDL: implications for LDL oxidative susceptibility. *Biochim. Biophys. Acta.* **1437:** 23–36.
49. Segrest, J. P., M. K. Jones, V. K. Mishra, G. M. Anantharamaiah, and D. W. Garber. 1994. ApoB-100 has a pentapartite structure composed of three amphipathic alpha-helical domains alternating with two amphipathic beta-strand domains. Detection by the computer program LOCATE. *Arterioscler. Thromb.* **14:** 1674–1685.
50. Wang, L., M. T. Walsh, and D. M. Small. 2006. Apolipoprotein B is conformationally flexible but anchored at a triolein/water interface: a possible model for lipoprotein surfaces. *Proc. Natl. Acad. Sci. USA.* **103:** 6871–6876.
51. Stafforini, D. M., L. W. Tjoelker, S. P. McCormick, D. Vaitkus, T. M. McIntyre, P. W. Gray, S. G. Young, and S. M. Prescott. 1999. Molecular basis of the interaction between plasma platelet-activating factor acetylhydrolase and low density lipoprotein. *J. Biol. Chem.* **274:** 7018–7024.
52. Spooner, P. J., D. L. Gantz, J. A. Hamilton, and D. M. Small. 1990. The distribution of oleic acid between chylomicron-like emulsions, phospholipid bilayers, and serum albumin. A model for fatty acid distribution between lipoproteins, membranes, and albumin. *J. Biol. Chem.* **265:** 12650–12655.